Ocean Engineering 37 (2010) 1111–1119

Contents lists available at ScienceDirect

Ocean Engineering

journal homepage: www.elsevier.com/locate/oceaneng

Practical control of underactuated ships

K.D. Do

School of Mechanical Engineering, The University of Western Australia, 35 Stirling Highway, Crawley, WA 6009, Australia

ARTICLE INFO

Article history:
Received 9 July 2009
Accepted 28 April 2010
Available online 15 May 2010

Keywords:
Underactuated ships
Practical control
Nonlinear control
Transverse function
Lyapunov direct method

ABSTRACT

This paper presents a design of global smooth controllers that achieve the practical stabilization of arbitrary reference trajectories, including fixed points and nonadmissible trajectories for underactuated ships. These ships do not have an independent actuator in the sway axis. The control design is based on several nonlinear coordinate changes, the transverse function approach, the back-stepping technique, the Lyapunov direct method, and utilization of the ship dynamics. Simulation results illustrate the effectiveness of the proposed control design.

1. Introduction

The problem of stabilizing an underactuated ship at a desired reference trajectory is an important issue in many offshore applications. This goal can be achieved by solving trajectory-tracking, path-following, path-tracking and stabilization problems, see Do and Pan (2009). The main difficulty with controlling an underactuated ship is that only the yaw and surge axes are directly actuated while the sway axis is not actuated. This configuration is by far most common among the marine surface vessels (Fossen, 2002). It is also well known that the ships in question are a class of underactuated mechanical systems with nonintegrable dynamics and which are not transformable into a driftless system, see Wichlund et al. (1995). An application of Brockett's (1983) theorem shows the nonexistence of pure-state feedbacks that are able to asymptotically stabilize an underactuated ship at a fixed point. Nevertheless, due to numerous important applications of the underactuated ships the control problem of these vessels has recently received a lot of attention from the control community.

By linearizing the ship dynamics, several linear controllers for path control were proposed in Papoulias and Oral (1995) and Papoulias (1994) where loss of stability due to linearization was analyzed. A continuous time-invariant controller was developed in Godhavn et al. (1998) to achieve global exponential position tracking for underactuated ships. However, the ship orientation was not controlled. Output redefinition, input–output linearization and sliding mode techniques were used in Zhang et al. (2000) to obtain a local asymptotic result on path tracking for underactuated ships using rudders. In Encarnacao et al. (2000), the path following errors were first described in the Serret–Frenet frame, then a local path following controller was designed under constant ocean current disturbances. An application of the recursive technique for standard chain form systems (Jiang and Nijmeijer, 1999) was used in Pettersen and Nijmeijer (2001) to provide a high-gain, local exponential tracking result. By applying a cascade approach, a global tracking result was obtained in Lefeber et al. (2003). Based on Lyapunov's direct method and the passivity approach, two tracking solutions were proposed in Jiang (2002). It is noted that in Jiang (2002), Lefeber et al. (2003) and Pettersen and Nijmeijer (2001), the yaw velocity was required to be nonzero. This restrictive assumption implies that a straight-line cannot be tracked. It seems that the first global way-point tracking controller was proposed in Pettersen and Lefeber (2001) to force an underactuated ship to track a straight-line (see also Do and Pan, 2003; Do et al., 2003 for robust and output feedback versions of straight-line following controllers). In Do et al. (2002a), a solution was proposed to solve the problem of trajectory tracking without imposing the requirement that yaw velocity be nonzero. In Do et al. (2002b), a single controller was proposed to solve both stabilization and tracking simultaneously, see also Do and Pan (2005) for an interesting solution on relaxing the limitation on nonzero off-diagonal terms in the aforementioned articles. The work in Behal et al. (2002), see also Dixon et al. (2001) is of a particular relevance to the work presented in this paper. The core of the work in Behal et al. (2002) is the nontrivial coordinate transformation that was used to transform the underactuated ship dynamics to a convenient form. However, it is noted that this coordinate transformation only works for spherical vessels. Relevant independent work also includes Toussaint et al. (2000a, b) and Sira-ramirez (1999) on local tracking control and differential flatness approach. An output maneuvering controller was proposed in Skjetne and Fossen

E-mail address: duc@mech.uwa.edu.au

0029-8018/$ - see front matter © 2010 Elsevier Ltd. All rights reserved.
doi:10.1016/j.oceaneng.2010.04.007

(2001) for a class of strict feedback nonlinear systems (Krstic et al., 1995) and applied to maneuver fully actuated ships.

In all the aforementioned papers on controlling an underactuated ship, either the reference trajectories are limited or the control design procedures are too complicated to make them suitable for an implementation in practice. For example, all attempts to achieve fast convergence and robust stability have failed—to our knowledge. Moreover, it has been shown that the more general problem of asymptotic stabilization of feasible trajectories in its full generality is essentially unsolvable in the sense that the search for a causal feedback control scheme capable of stabilizing "any" feasible reference trajectory for this type of system is impossible, Lizarraga (2004). Whatever the chosen control strategy there always exists a feasible trajectory that this control is unable to stabilize asymptotically, even though any feasible trajectory taken separately can be asymptotically stabilized. Finally, the problem of feedback stabilization of nonfeasible trajectories has seldom been addressed. The above theoretical obstructions and shortcomings motivate the contributions of this paper. This paper provides a solution for a control objective of global practical stabilization of arbitrary reference trajectories, including fixed points and nonadmissible trajectories for underactuated ships without an independent actuator in the sway axis. The proposed solution is based on several nonlinear coordinate changes, the transverse function approach in Morin and Samson (2001, 2003, 2006), a disturbance observer, Lyapunov direct method, and the backstepping technique found in Khalil (2002) and Krstic et al. (1995).

The rest of the paper is organized as follows. In the next section, the mathematical model of an underactuated ship moving in a horizontal plane under external disturbances induced by waves, wind, and ocean currents is derived, and the control objective is then formulated. In Section 3, a disturbance observer is constructed for a general nonlinear system. This disturbance observer is to be applied to provide an exponential estimate of the external disturbances in the ship model in Section 5. Section 4 presents two sets of coordinate transformations for preparation of the control design in Section 5. To overcome difficulties caused by nonzero off-diagonal terms in the system matrices, the first set of coordinate transformations changes the ship position such that the ship model is transformed to a diagonal form. The second set of coordinate transformations is applied to the transformed model with zero off-diagonal terms to provide a model of stabilizing/tracking errors' dynamics plus an "additional control input". The result of Section 4 is the model of the ship stabilizing/tracking errors in a strict feedback form Krstic et al. (1995). This form is very convenient for designing a control law. Section 5 details the design of a control law to stabilize the ship stabilizing/tracking errors at the origin using the disturbance observer constructed in Section 3, the Lyapunov direct method, and the backstepping technique. In Section 6, several simulations are provided to illustrate the effectiveness of the proposed controller. Section 7 gives concluding remarks of the paper. Finally, proof of the disturbance observer design and the main control design results is given in Appendices A and B, respectively.

2. Problem formulation

Assume that the ship has an xz-plane of symmetry; heave, pitch and roll modes are neglected; the body-fixed frame coordinate origin is set in the center-line of the ship. Then the mathematical model of an underactuated ship moving in a horizontal plane is described as (Fossen, 2002)

$$\dot{\boldsymbol{\eta}} = \boldsymbol{J}(\psi)\boldsymbol{\nu},$$

$$\boldsymbol{M}\dot{\boldsymbol{\nu}} = -\boldsymbol{C}(\boldsymbol{\nu})\boldsymbol{\nu} - \boldsymbol{D}(\boldsymbol{\nu})\boldsymbol{\nu} + \boldsymbol{\tau} + \boldsymbol{J}^{T}(\psi)\boldsymbol{b} \tag{1}$$

where $\boldsymbol{\eta} = [x\ y\ \psi]^T$ is the vector denoting the ship position (x,y) and yaw angle ψ with coordinates in the earth-fixed frame; $\boldsymbol{\nu} = [u\ v\ r]^T$ is the vector denoting the ship velocities (surge velocity: u, sway velocity: v, and yaw velocity: r) with coordinates in the body-fixed frame; $\boldsymbol{b} = [b_1\ b_2\ b_3]^T$ is the vector representing constant unmodeled external forces due to waves, wind, and ocean currents acting on the ship with coordinates in the earth-fixed frame; $\boldsymbol{\tau} = [\tau_u\ 0\ \tau_r]^T$ is the control vector of surge force τ_u, and yaw moment τ_r. The matrices $\boldsymbol{J}(\boldsymbol{\eta})$, $\boldsymbol{M}$, $\boldsymbol{C}(\boldsymbol{\nu})$ and $\boldsymbol{D}(\boldsymbol{\nu})$ are given below:

$$\boldsymbol{J}(\psi) = \begin{bmatrix} \cos(\psi) & -\sin(\psi) & 0 \\ \sin(\psi) & \cos(\psi) & 0 \\ 0 & 0 & 1 \end{bmatrix}, \quad \boldsymbol{D} = -\begin{bmatrix} d_{11}(u) & 0 & 0 \\ 0 & d_{22}(v,r) & d_{23}(v,r) \\ 0 & d_{32}(v,r) & d_{33}(v,r) \end{bmatrix},$$

$$\boldsymbol{C}(\boldsymbol{\nu}) = \begin{bmatrix} 0 & 0 & -m_{22}v - m_{23}r \\ 0 & 0 & m_{11}u \\ m_{22}v + m_{23}r & -m_{11}u & 0 \end{bmatrix}, \quad \boldsymbol{M} = \begin{bmatrix} m_{11} & 0 & 0 \\ 0 & m_{22} & m_{23} \\ 0 & m_{23} & m_{33} \end{bmatrix}, \tag{2}$$

where

$$m_{11} = m - X_{\dot{u}}, \quad m_{22} = m - Y_{\dot{v}}, \quad m_{23} = mx_g - Y_{\dot{r}}, \quad m_{33} = I_z - N_{\dot{r}},$$

$$d_{11}(u) = -(X_u + X_{u|u|}|u|), \quad d_{22}(v,r) = -(Y_v + Y_{|v|v}|v| + Y_{|r|v}|r|),$$

$$d_{23}(v,r) = -(Y_r + Y_{|v|r}|v| + Y_{|r|r}|r|), \quad d_{32}(v,r) = -(N_v + N_{|v|v}|v| + N_{|r|v}|r|),$$

$$d_{33}(v,r) = -(N_r + N_{|v|r}|v| + N_{|r|r}|r|). \tag{3}$$

In (3), m is the mass of the ship; I_z is the ship's inertia about the Z_b-axis of the body-fixed frame; x_g is the X_b-coordinate of the ship center of gravity (CG) in the body-fixed frame, see Fig. 1 (at the end of the paper); the other symbols are referred to as hydrodynamic derivatives, see SNAME (1950). For example, the hydrodynamic added mass force Y along the y-axis due to an acceleration $\dot{u}$ in the x-direction is written as $Y = -Y_{\dot{u}}\dot{u}$ with $Y_{\dot{u}} = \partial Y / \partial \dot{u}$.

In this paper, we consider a control objective to achieve the practical stabilization of arbitrary reference trajectories, including fixed points and nonadmissible trajectories for the position and orientation vector $\boldsymbol{\eta}$ of the underactuated ship with the dynamics given in (1) while keeping the ship velocity vector $\boldsymbol{\nu}$ bounded. In particular, for any initial conditions $\boldsymbol{\eta}(t_0) \in \mathbb{R}^3$ and $\boldsymbol{\nu}(t_0) \in \mathbb{R}^3$ at the initial time t_0 with $0 \le t_0 \le t$, and a twice differentiable reference trajectory vector $\boldsymbol{\eta_d}(t) = [x_d(t)\ y_d(t)\ \psi_d(t)]^T$, we will design the controls τ_u and τ_r to guarantee that

$$\lim_{t\to\infty} \|\boldsymbol{\eta}(t) - \boldsymbol{\eta_d}(t)\| = \mu_0,$$

$$\|\boldsymbol{\nu}(t)\| \le \nu_0, \tag{4}$$

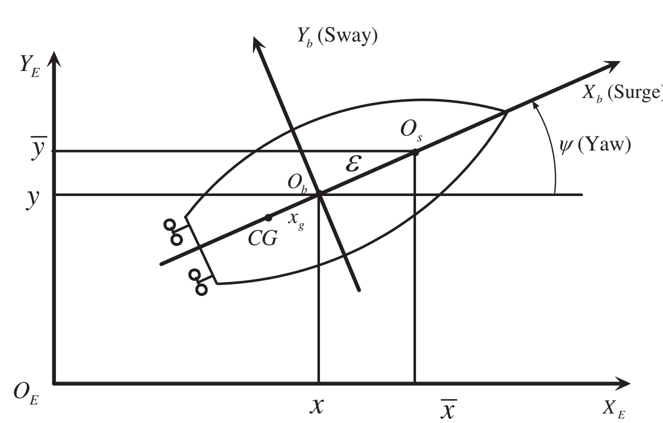

Fig. 1. Ship coordinates.

where μ_0 is a positive constant strictly larger than $|m_{23}/m_{22}|$, and v_0 is a nonnegative constant.

3. Disturbance observer

Since the ship dynamics (1) contain the unknown disturbance vector $\boldsymbol{b}$, we present in this section a disturbance observer for a general nonlinear system. This disturbance observer will be used to estimate the unknown disturbance vector $\boldsymbol{b}$ in Section 5. Consider the following system:

$$\dot{\boldsymbol{x}}_1 = \boldsymbol{F}_1(\boldsymbol{x}_1,\boldsymbol{x}_2),$$

$$\dot{\boldsymbol{x}}_2 = \boldsymbol{F}_2(\boldsymbol{x}_1,\boldsymbol{x}_2,\boldsymbol{u}) + \boldsymbol{G}(\boldsymbol{x}_1)\boldsymbol{d}(t), \tag{5}$$

where $\boldsymbol{x}_1 \in \mathbb{R}^{n_1}$ and $\boldsymbol{x}_2 \in \mathbb{R}^{n_2}$ are measurable states, $\boldsymbol{u} \in \mathbb{R}^m$ is the control input vector; $\boldsymbol{F}_1(\boldsymbol{x}_1,\boldsymbol{x}_2) \in \mathbb{R}^{n_1}$ is a vector of known functions of $\boldsymbol{x}_1$ and $\boldsymbol{x}_2$; $\boldsymbol{F}_2(\boldsymbol{x}_1,\boldsymbol{x}_2,\boldsymbol{u}) \in \mathbb{R}^{n_2}$ is a vector of known functions of $\boldsymbol{x}_1$, $\boldsymbol{x}_2$ and $\boldsymbol{u}$; $\boldsymbol{G}(\boldsymbol{x}_1) \in \mathbb{R}^{n_2\times n_2}$ is a known and invertible matrix for all $\boldsymbol{x}_1 \in \mathbb{R}^{n_1}$; and $\boldsymbol{d}(t) \in \mathbb{R}^{n_2}$ is a vector of unknown disturbances. We assume that there exists a nonnegative constant C_d such that $\|\dot{\boldsymbol{d}}(t)\| \le C_d$. Now we want to design the control input $\boldsymbol{u}$ to stabilize the system (5) at the origin. It is obvious that if we can design a disturbance observer, $\hat{\boldsymbol{d}}(t)$, that estimates $\boldsymbol{d}(t)$ sufficiently accurately, then depending on the structure of $\boldsymbol{F}_1(\boldsymbol{x}_1,\boldsymbol{x}_2)$ and $\boldsymbol{F}_2(\boldsymbol{x}_1,\boldsymbol{x}_2,\boldsymbol{u})$ the control input $\boldsymbol{u}$ can be designed based on the available techniques in Khalil (2002) and Krstic et al. (1995). Here, our interest is to design an observer that can estimate the disturbance vector $\boldsymbol{d}(t)$ in the following lemma.

Lemma 3.1. *Consider the following disturbance observer*:

$$\hat{\boldsymbol{d}}(t) = \xi + \boldsymbol{K}_0\boldsymbol{G}^{-1}(\boldsymbol{x}_1)\boldsymbol{x}_2,$$

$$\dot{\xi} = -\boldsymbol{K}_0\xi - \boldsymbol{K}_0(\dot{\boldsymbol{G}}^{-1}(\boldsymbol{x}_1)\boldsymbol{x}_2 + \boldsymbol{G}^{-1}(\boldsymbol{x}_1)\boldsymbol{F}_2(\boldsymbol{x}_1,\boldsymbol{x}_2,\boldsymbol{u}) + \boldsymbol{K}_0\boldsymbol{G}^{-1}(\boldsymbol{x}_1)\boldsymbol{x}_2), \tag{6}$$

where $\boldsymbol{K}_0$ is a positive definite symmetric matrix. Assume that the solutions of (5) *and* (6) *exist for all $t \ge t_0 \ge 0$ where t_0 is the initial time, the disturbance observer* (6) *guarantees that the disturbance observer error $\boldsymbol{d}_e(t) = \boldsymbol{d}(t) - \hat{\boldsymbol{d}}(t)$ exponentially converges to a ball centered at the origin. The radius of this ball can be made arbitrarily small by adjusting the matrix $\boldsymbol{K}_0$. In the case $C_d=0$, i.e., the disturbance vector $\boldsymbol{d}$ is constant, the disturbance observer error $\boldsymbol{d}_e(t)$ exponentially converges to zero.*

Proof. See Appendix A.

Remark 3.1. Existence of the solutions of (5) and (6) is to be guaranteed by a proper design of the control input u. The disturbance observer (6) is a dynamical system. The variable ξ is generated by the second equation of (6), which is an ordinary differential equation, with some initial value $\xi(t_0)$. The choice of the matrix $\boldsymbol{K}_0$ directly affects performance of the disturbance observer. The larger eigenvalues of the matrix $\boldsymbol{K}_0$ are the faster the response of the disturbance observer is with a trade-off of a large overshoot of the observer, and vice versa. The initial value $\xi(t_0)$ is ideally chosen to be $\boldsymbol{d}(t_0)\boldsymbol{K}_0\boldsymbol{G}^{-1}(\boldsymbol{x}_1(t_0))\boldsymbol{x}_2(t_0)$, where $\boldsymbol{d}(t_0)$ and $\boldsymbol{K}_0\boldsymbol{G}^{-1}(\boldsymbol{x}_1(t_0))\boldsymbol{x}_2(t_0)$ are the initial values of $\boldsymbol{d}(t)$ and $\boldsymbol{K}_0\boldsymbol{G}^{-1}(\boldsymbol{x}_1(t))\boldsymbol{x}_2(t_0)$, respectively. However, $\boldsymbol{d}(t_0)$ is unavailable since the disturbance $\boldsymbol{d}(t)$ is unknown, we usually take $\xi(t_0)=0$ in practice. Of course, one can choose $\xi(t_0)$ to be any constant but the transient response of the disturbance observer might be bad because as $\boldsymbol{d}(t_0)$ is unknown, the chosen constant $\xi(t_0)$ can make $\|\boldsymbol{d}(t_0) - \boldsymbol{K}_0\boldsymbol{G}^{-1}(\boldsymbol{x}_1(t_0))\boldsymbol{x}_2(t_0)\|$ large.

4. Coordinate transformations

4.1. Transform ship dynamics to a "diagonal form"

To avoid the yaw moment control τ_r acting directly on the sway dynamics caused by off-diagonal terms in the mass matrix, we introduce the following coordinate transformations (changing the ship position, see Fig. 1 (at the end of the paper):

$$\overline{x} = x + \varepsilon\cos(\psi),$$

$$\overline{y} = y + \varepsilon\sin(\psi),$$

$$\overline{v} = v + \varepsilon r, \tag{7}$$

where $\varepsilon = m_{23}/m_{22}$. Using the above change of coordinates, the ship dynamics (1) can be written as

$$\dot{\overline{x}} = u\cos(\psi) - \overline{v}\sin(\psi),$$

$$\dot{\overline{y}} = u\sin(\psi) + \overline{v}\cos(\psi),$$

$$\dot{\psi} = r,$$

$$\dot{u} = \varphi_u + \frac{1}{m_{11}}\tau_u + \frac{1}{m_{11}}(b_1\cos(\psi) + b_2\sin(\psi)),$$

$$\dot{\overline{v}} = \varphi_v + \frac{m_{23}}{m_{22}}\varphi_r + \frac{1}{m_{22}}(-b_1\sin(\psi) + b_2\cos(\psi)),$$

$$\dot{r} = \varphi_r + \frac{m_{22}}{\Delta}\tau_r + \frac{m_{23}}{\Delta}(b_1\sin(\psi) - b_2\cos(\psi)) + \frac{m_{22}}{\Delta}b_3, \tag{8}$$

where

$$\Delta = m_{22}m_{33} - m_{23}^2,$$

$$\varphi_u = \frac{m_{22}}{m_{11}}vr + \frac{m_{23}}{m_{11}}r^2 - \frac{d_{11}(u)}{m_{11}}u,$$

$$\varphi_v = -\frac{m_{11}}{m_{22}}ur - \frac{d_{22}(v,r)}{m_{22}}v - \frac{d_{23}(v,r)}{m_{22}}r,$$

$$\varphi_r = \frac{m_{11}m_{22} - m_{22}^2}{\Delta}uv + \frac{m_{11}m_{23} - m_{23}m_{22}}{\Delta}ur - \frac{m_{22}}{\Delta}(d_{33}(v,r)r + d_{32}(v,r)v) + \frac{m_{23}}{\Delta}(d_{23}(v,r)r + d_{22}(v,r)v). \tag{9}$$

It is clearly seen from (8) that the yaw moment control τ_r does not directly act on the $\overline{v}$−dynamics.

4.2. Transform ship dynamics to a form with an "additional control"

To overcome difficulties caused by the underactuation, we introduce the following coordinate transformations to provide an "additional control" $\dot{\alpha}$, see (14):

$$\boldsymbol{q} = \boldsymbol{R}(-\psi_d)\begin{bmatrix}\overline{x}\\ \overline{y}\end{bmatrix} - \boldsymbol{R}(\psi_e)\begin{bmatrix}f_1(\alpha)\\ f_2(\alpha)\end{bmatrix},$$

$$\boldsymbol{q}_d = \boldsymbol{R}(-\psi_d)\begin{bmatrix}x_d\\ y_d\end{bmatrix},$$

$$\psi_e = \psi - \psi_d - f_3(\alpha),$$

$$\boldsymbol{q}_e = \boldsymbol{q} - \boldsymbol{q}_d, \tag{10}$$

where $f_i(\alpha)$, $i=1, 2, 3$ are differentiable functions of α such that $|f_i(\alpha)| \le \gamma_i$ for all $\alpha \in \mathbb{R}$ with γ_i being a positive constant. These functions need to satisfy some further requirements, and are to be determined later. The rotational matrix $\boldsymbol{R}(\bullet)$ is given by

$$\boldsymbol{R}(\bullet)=\begin{bmatrix}\cos(\bullet) & -\sin(\bullet)\\ \sin(\bullet) & \cos(\bullet)\end{bmatrix}. \tag{11}$$

From the coordinate transformations given in (10), we have

$$\begin{bmatrix}\overline{x}-x_d\\ \overline{y}-y_d\end{bmatrix}=\boldsymbol{R}^{-1}(-\psi_d)\left(\boldsymbol{q_e}+\boldsymbol{R}(\psi_e)\begin{bmatrix}f_1(\alpha)\\ f_2(\alpha)\end{bmatrix}\right),$$
$$\psi-\psi_d=\psi_e+f_3(\alpha). \tag{12}$$

A simple calculation from (12) shows that

$$\|((\overline{x}-x_d),(\overline{y}-y_d))\|\le\|\boldsymbol{q_e}\|+\|(f_1(\alpha),f_2(\alpha))\|,$$
$$|\psi-\psi_d|\le|\psi_e|+|f_3(\alpha)|. \tag{13}$$

Because all the functions $f_i(\alpha)$ are bounded by γ_i for all $\alpha\in\mathbb{R}$ (these functions are to be determined later), the bounds in (13) mean that we just need to design control laws for τ_u and τ_r such that $\psi_e(t)$ and $\boldsymbol{q_e}(t)$ converge to zero, and all the ship velocities (u, v, r) are bounded. Then the control objective is solved. As such, differentiating both sides of the last two equations of (10) along the solutions of the first two equations of (10), and the first three equations of (8) and combining the last three equations of (8) give

$$\dot{\boldsymbol{q}}_{\boldsymbol{e}}=\boldsymbol{Q}\begin{bmatrix}u\\ \dot{\alpha}\end{bmatrix}+\boldsymbol{\Delta}_1+\boldsymbol{\Delta}_2\dot{\psi}_e-\dot{\boldsymbol{q}}_{\boldsymbol{d}},$$
$$\dot{\psi}_e=r-\dot{\psi}_d-f_3'\dot{\alpha},$$
$$\dot{u}=\varphi_u+\frac{1}{m_{11}}\tau_u+\frac{1}{m_{11}}(b_1\cos(\psi)+b_2\sin(\psi)),$$
$$\dot{\overline{v}}=\varphi_v+\frac{m_{23}}{m_{22}}\varphi_r+\frac{1}{m_{22}}(-b_1\sin(\psi)+b_2\cos(\psi)),$$
$$\dot{r}=\varphi_r+\frac{m_{22}}{\Delta}\tau_r+\frac{m_{23}}{\Delta}(b_1\sin(\psi)-b_2\cos(\psi))+\frac{m_{22}}{\Delta}b_3, \tag{14}$$

where $f_3'=\partial f_3/\partial\alpha$, and

$$\boldsymbol{Q}=\left[\boldsymbol{R}(-\psi_d)\begin{bmatrix}\cos(\psi)\\ \sin(\psi)\end{bmatrix}\;-\boldsymbol{R}(\psi_e)\begin{bmatrix}f_1'\\ f_2'\end{bmatrix}\right],$$
$$\boldsymbol{\Delta}_1=\boldsymbol{R}(-\psi_d)\begin{bmatrix}-\overline{v}\sin(\psi)\\ \overline{v}\cos(\psi)\end{bmatrix}+\dot{\boldsymbol{R}}(-\psi_d)\begin{bmatrix}\overline{x}\\ \overline{y}\end{bmatrix},\quad \boldsymbol{\Delta}_2=-\overline{\boldsymbol{R}}(\psi_e)\begin{bmatrix}f_1\\ f_2\end{bmatrix}, \tag{15}$$

with $f_i'=\partial f_i/\partial\alpha$, $i=1$, 2 and

$$\overline{\boldsymbol{R}}(\bullet)=\begin{bmatrix}-\sin(\bullet) & -\cos(\bullet)\\ \cos(\bullet) & -\sin(\bullet)\end{bmatrix}. \tag{16}$$

To prepare for the control design in the next section, we now specify the functions $f_i(\alpha)$, $i=1$, 2, 3 such that they are bounded, differentiable and make the matrix $\boldsymbol{Q}$ invertible. Expanding the first equation of (15) gives

$$\boldsymbol{Q}=\begin{bmatrix}\cos(\psi-\psi_d) & -\cos(\psi_e)f_1'+\sin(\psi_e)f_2'\\ \sin(\psi-\psi_d) & -\sin(\psi_e)f_1'-\cos(\psi_e)f_2'\end{bmatrix}, \tag{17}$$

where we have dropped the argument α of the functions $f_i(\alpha)$ for clarity. Therefore, the determinant of the matrix $\boldsymbol{Q}$ is

$$\det(\boldsymbol{Q})=\sin(f_3)f_1'-\cos(f_3)f_2'. \tag{18}$$

A nontrivial choice of the functions f_i that are bounded, differentiable and make $\det(\boldsymbol{Q})$ nonzero for all $\alpha\in\mathbb{R}$ is

$$f_1=\varepsilon_1\sin(\alpha)\frac{\sin(f_3)}{f_3},$$
$$f_2=\varepsilon_1\sin(\alpha)\frac{1-\cos(f_3)}{f_3},$$
$$f_3=\varepsilon_2\cos(\alpha), \tag{19}$$

where the constants ε_1 and ε_2 are chosen such that

$$\varepsilon_1>0,$$
$$0<\varepsilon_2<\frac{\pi}{2}. \tag{20}$$

With the above choice of f_i in (19), a simple calculation shows that

$$|f_1|\le\varepsilon_1,\quad |f_2|\le\varepsilon_1,\quad |f_3|\le\varepsilon_2,$$
$$\det(\boldsymbol{Q})=-\frac{\varepsilon_1\varepsilon_2}{(\varepsilon_2\cos(\alpha))^2}(\cos(\varepsilon_2\cos(\alpha))-1)$$
$$\Rightarrow\quad |\det(\boldsymbol{Q})|\ge\frac{\varepsilon_1}{\varepsilon_2}(1-\cos(\varepsilon_2)). \tag{21}$$

We also calculate the inverse of the matrix $\boldsymbol{Q}$ to be used in the next section as follows:

$$\boldsymbol{Q}^{-1}=\frac{1}{\det(\boldsymbol{Q})}\begin{bmatrix}-\sin(\psi_e)f_1'-\cos(\psi_e)f_2' & \cos(\psi_e)f_1'-\sin(\psi_e)f_2'\\ -\sin(\psi-\psi_d) & \cos(\psi-\psi_d)\end{bmatrix}. \tag{22}$$

5. Control design

A close look at the system (14) shows that this system is of a strict feedback form. Therefore, we will apply the Lyapunov direct method and the backstepping technique to design the controls τ_u and τ_r to globally asymptotically stabilize the system (14) at the origin. As such, the control design consists of two steps. In the first step, the first two equations of (14) are considered using u, $\dot{\alpha}$ and r as controls to stabilize $\boldsymbol{q_e}$ and ψ_e at the origin. In the second step, the actual controls τ_u and τ_r are designed to stabilize the difference between u and r, and their virtual controls at the origin. In this step, the disturbance observer in Section 3 is used to estimate the disturbance vector $\boldsymbol{b}$.

5.1. Step 1

Define the following errors:

$$u_e=u-\beta_u,$$
$$r_e=r-\beta_r, \tag{23}$$

where β_u and β_r are virtual controls of u and r, respectively. To design the virtual controls β_u and β_r, we consider the following Lyapunov function candidate:

$$V_1=\tfrac{1}{2}\boldsymbol{q_e^T}\boldsymbol{q_e}+\tfrac{1}{2}\psi_e^2. \tag{24}$$

Differentiating both sides of (24) along the solutions of the first two equations of (14) results in

$$\dot{V}_1=\boldsymbol{q_e^T}\left(\boldsymbol{Q}\begin{bmatrix}\beta_u+u_e\\ \dot{\alpha}\end{bmatrix}+\boldsymbol{\Delta}_1+\boldsymbol{\Delta}_2\dot{\psi}_e-\dot{\boldsymbol{q}}_{\boldsymbol{d}}\right)+\psi_e(\beta_r+r_e-\dot{\psi}_d-f_3'\dot{\alpha}). \tag{25}$$

From (25), we choose the virtual controls β_u, β_r, and the additional control $\dot{\alpha}$ as

$$\begin{bmatrix}\beta_u\\ \dot{\alpha},\end{bmatrix}=\boldsymbol{Q}^{-1}(-\boldsymbol{K_1}\boldsymbol{q_e}+\dot{\boldsymbol{q}}_{\boldsymbol{d}}-\boldsymbol{\Delta_1}),$$
$$\beta_r=-k_2\psi_e+\dot{\psi}_d+f_3'\dot{\alpha}, \tag{26}$$

where $\boldsymbol{K_1}$ is a positive definite symmetric matrix, and k_2 is a positive constant. Substituting the choice of the virtual controls β_u, β_r, and the additional control $\dot{\alpha}$ into (25) gives

$$\dot{V}_1=-\boldsymbol{q_e^T}\boldsymbol{K_1}\boldsymbol{q_e}-k_2\psi_e^2+\boldsymbol{q_e^T}\left(\boldsymbol{Q}\begin{bmatrix}u_e\\ 0\end{bmatrix}-k_2\boldsymbol{\Delta}_2\psi_e\right)+r_e(\psi_e+\boldsymbol{q_e^T}\boldsymbol{\Delta_2}). \tag{27}$$

Moreover, substituting the choice of the virtual controls β_u, β_r, and the additional control $\dot{\alpha}$ into the first two equations of (14) results in

$$\dot{\boldsymbol{q}}_{\boldsymbol{e}} = -\boldsymbol{K_1}\boldsymbol{q_e} + \boldsymbol{Q}\begin{bmatrix} u_e \\ 0 \end{bmatrix} + \boldsymbol{\Delta}_2(-k_2\psi_e + r_e),$$

$$\dot{\psi}_e = -k_2\psi_e + r_e. \tag{28}$$

It is noted from (26) that the virtual controls β_u, β_r, and the additional control $\dot{\alpha}$ are differentiable functions of $\boldsymbol{q_e}$, $\dot{\boldsymbol{q}}_{\boldsymbol{d}}$, ψ_d, $\dot{\psi}_d$, ψ, $\overline{v}$, $\overline{x}$, $\overline{y}$ and α.

5.2. Step 2

In this step, we design the actual controls τ_u and τ_r. As mentioned earlier, we now apply the disturbance observer in Section 3 to (8). It is noted that we can apply the disturbance observer in Section 3 to (14). However, we use (8) to design a disturbance observer for $\boldsymbol{b}$ for simplicity of presentation. As such, it is not hard to see that (8) is of the form (5) with

$$\boldsymbol{x_1} = \begin{bmatrix} \overline{x} \\ \overline{y} \\ \psi \end{bmatrix}, \quad \boldsymbol{x_2} = \begin{bmatrix} u \\ \overline{v} \\ r \end{bmatrix}, \quad \boldsymbol{F_1}(\boldsymbol{x_1},\boldsymbol{x_2}) = \begin{bmatrix} u\cos(\psi) - \overline{v}\sin(\psi) \\ u\sin(\psi) + \overline{v}\cos(\psi) \\ r \end{bmatrix},$$

$$\boldsymbol{F_2}(\boldsymbol{x_1},\boldsymbol{x_2},\boldsymbol{u}) = \begin{bmatrix} \varphi_u + \dfrac{1}{m_{11}}\tau_u \\ \varphi_v + \dfrac{m_{23}}{m_{22}}\varphi_r \\ \varphi_r + \dfrac{m_{22}}{\Delta}\tau_r \end{bmatrix},$$

$$\boldsymbol{G}(\boldsymbol{x_1}) = \begin{bmatrix} \dfrac{1}{m_{11}}\cos(\psi) & \dfrac{1}{m_{11}}\sin(\psi) & 0 \\ -\dfrac{1}{m_{22}}\sin(\psi) & \dfrac{1}{m_{22}}\cos(\psi) & 0 \\ \dfrac{m_{23}}{\Delta}\sin(\psi) & -\dfrac{m_{23}}{\Delta}\cos(\psi) & \dfrac{m_{22}}{\Delta} \end{bmatrix}. \tag{29}$$

Clearly the matrix $\boldsymbol{G}(\boldsymbol{x_1})$ is invertible for all $\psi \in \mathbb{R}$ since its determinant is $\det(\boldsymbol{G}(\boldsymbol{x_1})) = 1/m_{11}\Delta$. Therefore, we can directly apply the disturbance observer in Section 3 to (14) to estimate the disturbance vector $\boldsymbol{b}$ as follows:

$$\hat{\boldsymbol{b}} = \xi + \boldsymbol{K_0}\boldsymbol{G}^{-1}(\boldsymbol{x_1})\boldsymbol{x_2},$$

$$\dot{\xi} = -\boldsymbol{K}_0\xi - \boldsymbol{K}_0(\dot{\boldsymbol{G}}^{-1}(\boldsymbol{x_1})\boldsymbol{x_2} + \boldsymbol{G}^{-1}(\boldsymbol{x_1})\boldsymbol{F}_2(\boldsymbol{x_1},\boldsymbol{x_2},\boldsymbol{u}) + \boldsymbol{K_0}\boldsymbol{G}^{-1}(\boldsymbol{x_1})\boldsymbol{x_2}), \tag{30}$$

where $\boldsymbol{x_1}$, $\boldsymbol{x_2}$, $\boldsymbol{F_1}(\boldsymbol{x_1},\boldsymbol{x_2})$, $\boldsymbol{F_2}(\boldsymbol{x_1},\boldsymbol{x_2},\boldsymbol{u})$ and $\boldsymbol{G_1}(\boldsymbol{x_1})$ are given in (29), and $\boldsymbol{K_0}$ is a positive definite symmetric matrix. Indeed, differentiating both sides of $\boldsymbol{b_e} = \boldsymbol{b} - \hat{\boldsymbol{b}}$ along the solutions of (30) gives

$$\dot{\boldsymbol{b}}_{\boldsymbol{e}} = -\boldsymbol{K_0}\boldsymbol{b_e}, \tag{31}$$

where we have used $\dot{\boldsymbol{b}} = 0$ since $\boldsymbol{b}$ is a constant vector. Now differentiating both sides of (23) along the solutions of (14) results in

$$\begin{aligned}\dot{u}_e = {} & \varphi_u + \frac{1}{m_{11}}\tau_u + \frac{1}{m_{11}}(b_1\cos(\psi) + b_2\sin(\psi)) \\ & - \frac{\partial\beta_u}{\partial\boldsymbol{q_e}}\left(-\boldsymbol{K_1}\boldsymbol{q_e} + \boldsymbol{Q}\begin{bmatrix} u_e \\ 0 \end{bmatrix} + \boldsymbol{\Delta}_2(-k_2\psi_e + r_e)\right) - \frac{\partial\beta_u}{\partial\dot{\boldsymbol{q}}_{\boldsymbol{d}}}\ddot{\boldsymbol{q}}_{\boldsymbol{d}} - \frac{\partial\beta_u}{\partial\psi_d}\dot{\psi}_d \\ & - \frac{\partial\beta_u}{\partial\dot{\psi}_d}\ddot{\psi}_d - \frac{\partial\beta_u}{\partial\overline{x}}(u\cos(\psi) - \overline{v}\sin(\psi)) - \frac{\partial\beta_u}{\partial\overline{y}}(u\sin(\psi) + \overline{v}\cos(\psi)) \\ & - \frac{\partial\beta_u}{\partial\alpha}\dot{\alpha} - \frac{\partial\beta_u}{\partial\overline{v}}\left(\varphi_v + \frac{m_{23}}{m_{22}}\varphi_r + \frac{1}{m_{22}}(-b_1\sin(\psi) + b_2\cos(\psi))\right),\end{aligned}$$

$$\begin{aligned}\dot{r}_e = {} & \varphi_r + \frac{m_{22}}{\Delta}\tau_r + \frac{m_{23}}{\Delta}(b_1\sin(\psi) - b_2\cos(\psi)) + \frac{m_{22}}{\Delta}b_3 \\ & - \frac{\partial\beta_r}{\partial\boldsymbol{q_e}}\left(-\boldsymbol{K_1}\boldsymbol{q_e} + \boldsymbol{Q}\begin{bmatrix} u_e \\ 0 \end{bmatrix} + \boldsymbol{\Delta}_2(-k_2\psi_e + r_e)\right) - \frac{\partial\beta_r}{\partial\dot{\boldsymbol{q}}_{\boldsymbol{d}}}\ddot{\boldsymbol{q}}_{\boldsymbol{d}} - \frac{\partial\beta_r}{\partial\psi_d}\dot{\psi}_d \\ & - \frac{\partial\beta_r}{\partial\dot{\psi}_d}\ddot{\psi}_d - \frac{\partial\beta_r}{\partial\overline{x}}(u\cos(\psi) - \overline{v}\sin(\psi)) - \frac{\partial\beta_r}{\partial\overline{y}}(u\sin(\psi) + \overline{v}\cos(\psi)) \\ & - \frac{\partial\beta_r}{\partial\alpha}\dot{\alpha} - \frac{\partial\beta_r}{\partial\overline{v}}\left(\varphi_v + \frac{m_{23}}{m_{22}}\varphi_r + \frac{1}{m_{22}}(-b_1\sin(\psi) + b_2\cos(\psi))\right),\end{aligned} \tag{32}$$

where $\dot{\alpha}$ is given in (26). To design the actual controls τ_u and τ_r, we consider the following Lyapunov function candidate:

$$V_2 = V_1 + \tfrac{1}{2}u_e^2 + \tfrac{1}{2}r_e^2. \tag{33}$$

By taking the first time derivative of (33) along the solutions of (27) and (32), we choose the actual controls τ_u and τ_r as follows:

$$\begin{aligned}\tau_u = m_{11}\Bigg(& -\Bigg[\varphi_u + \frac{1}{m_{11}}(\hat{b}_1\cos(\psi) + \hat{b}_2\sin(\psi)) - \frac{\partial\beta_u}{\partial\boldsymbol{q_e}}\left(-\boldsymbol{K_1}\boldsymbol{q_e} + \boldsymbol{Q}\begin{bmatrix} u_e \\ 0 \end{bmatrix}\right. \\ & \left. + \boldsymbol{\Delta}_2(-k_2\psi_e + r_e)\right) - \frac{\partial\beta_u}{\partial\dot{\boldsymbol{q}}_{\boldsymbol{d}}}\ddot{\boldsymbol{q}}_{\boldsymbol{d}} - \frac{\partial\beta_u}{\partial\psi_d}\dot{\psi}_d - \frac{\partial\beta_u}{\partial\dot{\psi}_d}\ddot{\psi}_d \\ & - \frac{\partial\beta_u}{\partial\overline{x}}(u\cos(\psi) - \overline{v}\sin(\psi)) - \frac{\partial\beta_u}{\partial\overline{y}}(u\sin(\psi) + \overline{v}\cos(\psi)) - \frac{\partial\beta_u}{\partial\alpha}\dot{\alpha} \\ & - \frac{\partial\beta_u}{\partial\overline{v}}\left(\varphi_v + \frac{m_{23}}{m_{22}}\varphi_r + \frac{1}{m_{22}}(-\hat{b}_1\sin(\psi) + \hat{b}_2\cos(\psi))\right)\Bigg] \\ & - \boldsymbol{q_e^T}\boldsymbol{Q}\begin{bmatrix} 1 \\ 0 \end{bmatrix} - k_3u_e - \rho_3\left(\frac{\partial\beta_u}{\partial\overline{v}}\right)^2 u_e\Bigg),\end{aligned}$$

$$\begin{aligned}\tau_r = \frac{\Delta}{m_{22}}\Bigg(& -\Bigg[\varphi_r + \frac{m_{23}}{\Delta}(\hat{b}_1\sin(\psi) - \hat{b}_2\cos(\psi)) + \frac{m_{22}}{\Delta}\hat{b}_3 \\ & - \frac{\partial\beta_r}{\partial\boldsymbol{q_e}}\left(-\boldsymbol{K_1}\boldsymbol{q_e} + \boldsymbol{Q}\begin{bmatrix} u_e \\ 0 \end{bmatrix} + \boldsymbol{\Delta}_2(-k_2\psi_e + r_e)\right) - \frac{\partial\beta_r}{\partial\dot{\boldsymbol{q}}_{\boldsymbol{d}}}\ddot{\boldsymbol{q}}_{\boldsymbol{d}} - \frac{\partial\beta_r}{\partial\psi_d}\dot{\psi}_d \\ & - \frac{\partial\beta_r}{\partial\dot{\psi}_d}\ddot{\psi}_d - \frac{\partial\beta_r}{\partial\overline{x}}(u\cos(\psi) - \overline{v}\sin(\psi)) - \frac{\partial\beta_r}{\partial\overline{y}}(u\sin(\psi) + \overline{v}\cos(\psi)) \\ & - \frac{\partial\beta_r}{\partial\alpha}\dot{\alpha} - \frac{\partial\beta_r}{\partial\overline{v}}\left(\varphi_v + \frac{m_{23}}{m_{22}}\varphi_r + \frac{1}{m_{22}}(-\hat{b}_1\sin(\psi) + \hat{b}_2\cos(\psi))\right)\Bigg] \\ & - (\psi_e + \boldsymbol{q_e^T}\boldsymbol{\Delta_2}) - k_4r_e - \rho_4\left(\frac{\partial\beta_r}{\partial\overline{v}}\right)^2 r_e\Bigg),\end{aligned} \tag{34}$$

where k_3, k_4, ρ_3 and ρ_4 are positive constants; $\hat{b}_1$, $\hat{b}_2$ and $\hat{b}_3$ are defined by $\hat{\boldsymbol{b}} = [\hat{b}_1\ \hat{b}_2\ \hat{b}_3]^T$. The nonlinear damping terms $\rho_3(\partial\beta_u/\partial\overline{v})^2u_e$ and $\rho_4(\partial\beta_r/\partial\overline{v})^2r_e$ are included in the controls τ_u and τ_r, respectively, to prevent possible destabilization cause by the disturbance observer errors b_{1e} and b_{2e}, which are defined by $\boldsymbol{b_e} = [b_{1e}\ b_{2e}\ b_{3e}]^T$.

Substituting (34) into the first time derivative of V_2 results in

$$\begin{aligned}\dot{V}_2 = {} & -\boldsymbol{q_e^T}\boldsymbol{K_1}\boldsymbol{q_e} - k_2\psi_e^2 - k_2\boldsymbol{q_e^T}\boldsymbol{\Delta_2}\psi_e - k_3u_e^2 - \rho_3\left(\frac{\partial\beta_u}{\partial\overline{v}}\right)^2 u_e^2 - k_4r_e^2 \\ & - \rho_4\left(\frac{\partial\beta_r}{\partial\overline{v}}\right)^2 r_e^2 + \frac{u_e}{m_{11}}(b_{1e}\cos(\psi) + b_{2e}\sin(\psi)) \\ & - \frac{\partial\beta_u}{\partial\overline{v}}\frac{u_e}{m_{22}}(-b_{1e}\sin(\psi) + b_{2e}\cos(\psi)) + \frac{m_{23}r_e}{\Delta}(b_{1e}\sin(\psi) \\ & - b_{2e}\cos(\psi)) + \frac{m_{22}r_e}{\Delta}b_{3e} - \frac{\partial\beta_r}{\partial\overline{v}}\frac{r_e}{m_{22}}(-b_{1e}\sin(\psi) + b_{2e}\cos(\psi)).\end{aligned} \tag{35}$$

On the other hand, substituting (34) into (32) gives

$$\begin{aligned}\dot{u}_e = {} & -\boldsymbol{q_e^T}\boldsymbol{Q}\begin{bmatrix} 1 \\ 0 \end{bmatrix} - k_3u_e - \rho_3\left(\frac{\partial\beta_u}{\partial\overline{v}}\right)^2 u_e + \frac{1}{m_{11}}(b_{1e}\cos(\psi) + b_{2e}\sin(\psi)) \\ & - \frac{\partial\beta_u}{\partial\overline{v}}\frac{1}{m_{22}}(-b_{1e}\sin(\psi) + b_{2e}\cos(\psi)),\end{aligned}$$

$$r_e = -(\psi_e + \boldsymbol{q}_e^T \boldsymbol{\Delta}_2) - k_4 r_e - \rho_4 \left(\frac{\partial \beta_r}{\partial \bar{v}}\right)^2 r_e + \frac{m_{23}}{\Delta}(b_{1e}\sin(\psi) - b_{2e}\cos(\psi))$$
$$+ \frac{m_{22}}{\Delta} b_{3e} - \frac{\partial \beta_r}{\partial \bar{v}} \frac{1}{m_{22}}(-b_{1e}\sin(\psi) + b_{2e}\cos(\psi)). \tag{36}$$

We now present the main result of our paper in the following theorem.

Theorem 5.1. *The controls τ_u and τ_r given in* (34) *together with the disturbance observer given in* (30) *achieve the practical stabilization of arbitrary reference trajectories, including fixed points and nonadmissible trajectories for the position and orientation vector $\boldsymbol{\eta}$ of the underactuated ship with the dynamics given in* (1) *while guaranteeing the ship velocity vector $\boldsymbol{v}$ bounded. In particular, for any initial conditions $\boldsymbol{\eta}(t_0) \in \mathbb{R}^3$ and $\boldsymbol{v}(t_0) \in \mathbb{R}^3$ at the initial time t_0 with $0 \le t_0 \le t$, and a twice differentiable reference trajectory vector $\boldsymbol{\eta_d}(t) = [x_d(t)\ y_d(t)\ \psi_d(t)]^T$, the controls τ_u and τ_r given in* (34) *together with the disturbance observer given in* (30) *ensure that*

$$\lim_{t\to\infty} \|\boldsymbol{\eta}(t) - \boldsymbol{\eta_d}(t)\| = \mu_0,$$

$$\|\boldsymbol{v}(t)\| \le v_0, \tag{37}$$

where μ_0 is a positive constant strictly larger than $|m_{23}/m_{22}|$ and v_0 is a nonnegative constant.

Proof. See Appendix B.

6. Simulations

We perform some simulations to illustrate the effectiveness of our proposed controller on a container ship. The nondimensional parameters of the ship taken from Perez and Blanke (2002) are given in Table 1 (at the end of the paper). The control and disturbance observer gains are chosen as $\varepsilon_1 = 0.2$, $\varepsilon_2 = 0.1$, $\boldsymbol{K_1} = \left[\begin{smallmatrix} 2 & 0 \\ 0 & 2 \end{smallmatrix}\right]$, $k_2 = 2$, $k_3 = 4$, $k_4 = 4$, $\rho_3 = 0.1$, $\rho_4 = 0.1$. It can be readily checked that the above choice of the control and disturbance observer gains satisfies the condition (B.11). The reference trajectory $\boldsymbol{\eta_d}$ is generated by a virtual mobile robot as

$$\dot{\boldsymbol{\eta}}_{\boldsymbol{d}} = \begin{bmatrix} \cos(\psi_d) & 0 \\ \sin(\psi_d) & 0 \\ 0 & 1 \end{bmatrix} \begin{bmatrix} u_d \\ r_d \end{bmatrix}, \tag{38}$$

Table 1
Ship parameters for simulations.

Parameter	Value
m	750.81×10^{-5}
I_z	43.25×10^{-5}
$Y_{\dot{v}}$	-878×10^{-5}
$N_{\dot{r}}$	-30×10^{-5}
$X_{\vert u\vert u}$	-64.4×10^{-5}
$Y_{\vert v\vert v}$	-5801.5×10^{-5}
Y_r	118.2×10^{-5}
$Y_{\vert r\vert r}$	0
$N_{\vert v\vert v}$	-712.9×10^{-5}
N_r	0
$N_{\vert r\vert r}$	0
x_g	-0.46×10^{-5}
$X_{\dot{u}}$	-124.4×10^{-5}
$Y_{\dot{r}}$	-48.1×10^{-5}
X_u	-226.5×10^{-5}
Y_v	-725×10^{-5}
$Y_{\vert r\vert v}$	-1192.7×10^{-5}
$Y_{\vert v\vert r}$	-409.4×10^{-5}
N_v	-300×10^{-5}
$N_{\vert r\vert v}$	-174.7×10^{-5}
$N_{\vert v\vert r}$	-778.8×10^{-5}

with $\boldsymbol{\eta_d} = [x_d\ y_d\ \psi_d]^T$ and $\boldsymbol{\eta_d}(\mathbf{0}) = [0\ 0\ 0]^T$. We simulate for two cases of reference trajectories. For the first case, the reference velocities are chosen as $u_d = 5$ and $r_d = 0$, i.e., the reference trajectory is a straight-line, for the first 280 s, then $u_d = 5$ and $r_d = 0.5$, i.e. the reference trajectory is a circle, for the rest of the simulation time. For this case, the initial conditions are taken as $\boldsymbol{\eta} = [-5\ 5\ 0]^T$, $\boldsymbol{v} = [0\ 0\ 0]^T$ and $\boldsymbol{\xi} = [0\ 0\ 0]^T$. Simulation results are plotted in Fig. 2 (at the end of the paper). For a comparison, the universal time-varying controller proposed in Do et al. (2002b) is also simulated. The results are plotted in Fig. 3 (at the end of the paper). It is seen that the proposed controller in Do et al. (2002b) yields slightly worse performance than the one proposed in this paper due to the time-varying sinusoidal effect for this tracking case. It is noted that the universal time-varying controller proposed in Do et al. (2002b) involves a very complicated procedure of choosing the control gains.

For the second case, the reference velocities are chosen as $u_d = 0$ and $r_d = 0$, i.e., the reference trajectory is a point at the origin meaning that we simulate a stabilization problem. For this case, the initial conditions are taken as $\boldsymbol{\eta} = [-15\ 5\ 0]^T$, $\boldsymbol{v} = [0\ 0\ 0]^T$ and $\boldsymbol{\xi} = [0\ 0\ 0]^T$. Simulation results are plotted in Fig. 4 (at the end of the paper). The universal time-varying controller proposed in Do et al. (2002b) is also simulated for this case. The results are plotted in Fig. 5 (at the end of the paper). It is clearly seen from Figs. 4 and 5 that the controller proposed in this paper yields much better performance than the one in Do et al. (2002b) although the one in Do et al. (2002b) requires a very time-consuming procedure of choosing the control gains.

In summary, from Figs. 2 and 4, we can see that the proposed controller and disturbance observer in this paper provided acceptable results as proven in Theorem 5.1. The tracking and stabilization errors converge to a small ball centered at the origin while the disturbance observer errors exponentially converge to zero.

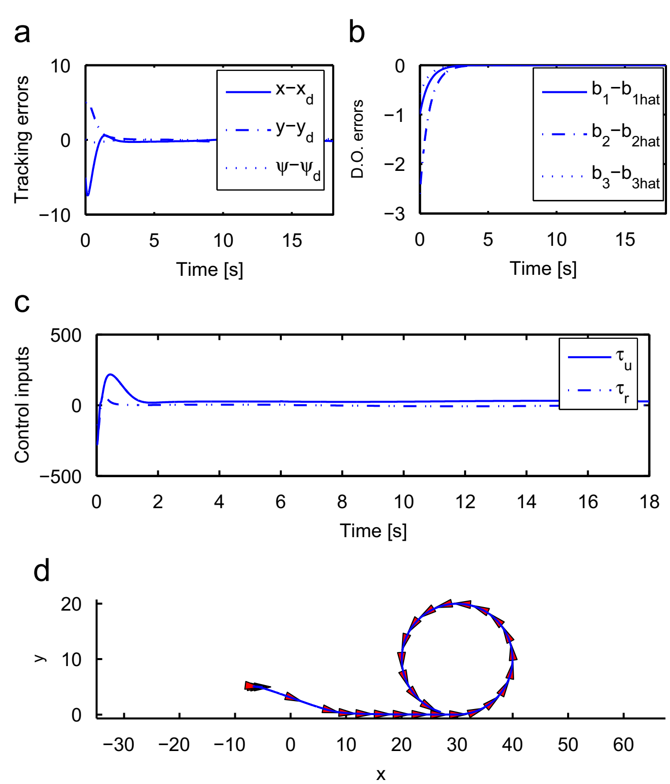

Fig. 2. Tracking simulation results by the controller in this paper: (a) tracking errors; (b) disturbance observer errors; (c) control inputs; (d) ship position and orientation in (x, y) plane.

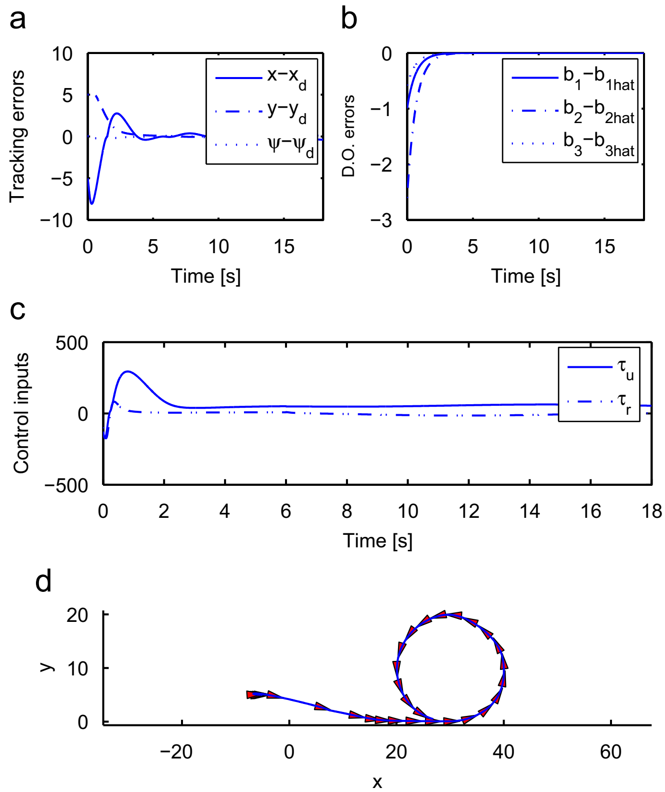

Fig. 3. Tracking simulation results by the controller in Do et al. (2002b): (a) tracking errors; (b) disturbance observer errors; (c) control inputs; (d) ship position and orientation in (x, y) plane.

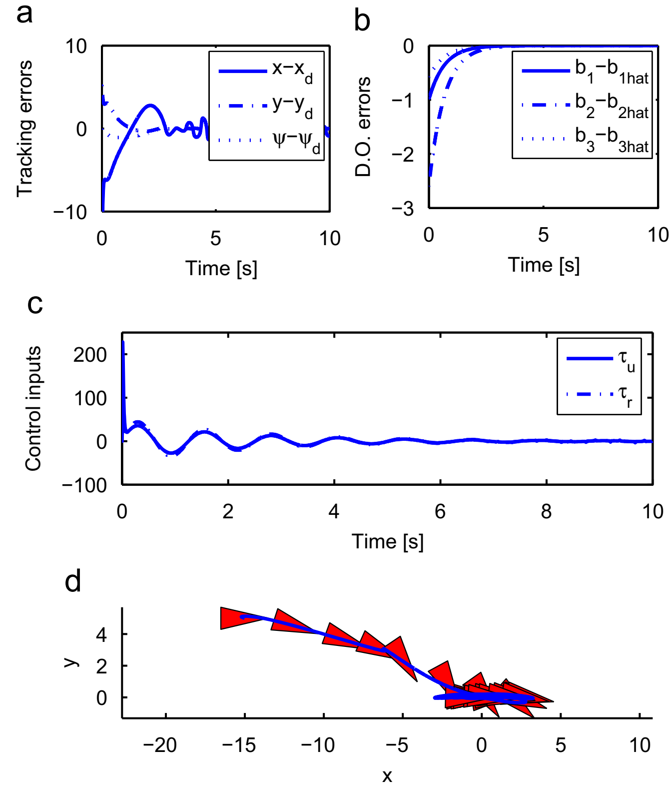

Fig. 5. Stabilization simulation results by the controller in Do et al. (2002b): (a) tracking errors; (b) disturbance observer errors; (c) control inputs; (d) ship position and orientation in (x, y) plane.

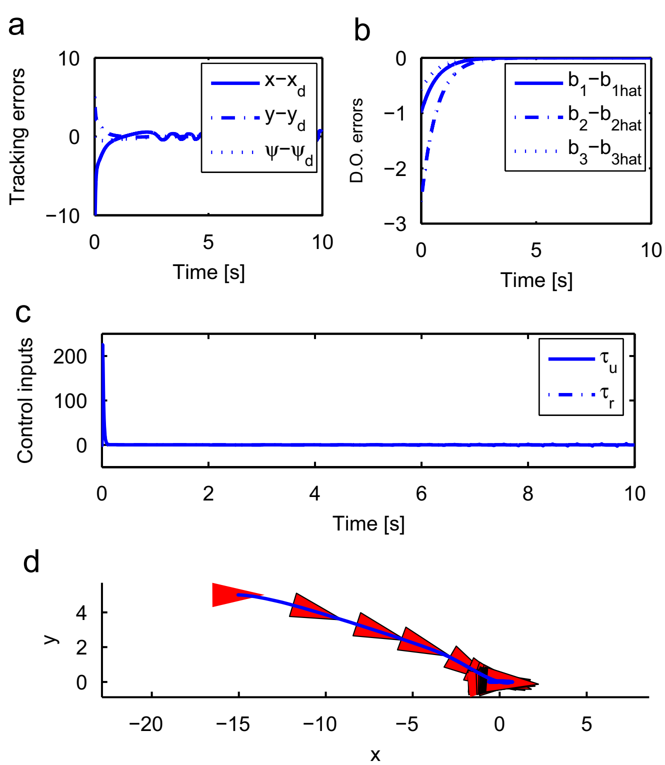

Fig. 4. Stabilization simulation results by the controller in this paper: (a) tracking errors; (b) disturbance observer errors; (c) control inputs; (d) ship position and orientation in (x, y) plane.

7. Conclusions

A method to design of global smooth controllers that achieve the practical stabilization of arbitrary reference trajectories, including fixed points and nonadmissible trajectories for under-actuated ships has been presented. In contrast with other methods dedicated to the stabilization of particular trajectories—fixed points and persistent feasible trajectories, see Section 1, the approach proposed in this paper aims at achieving the practical—by opposition to asymptotic-stabilization of reference trajectories regardless of their admissibility, and simplicity for an implementation in practice.

Appendix A. Proof of Lemma 3.1

To prove Lemma 3.1, let us first calculate the derivative of $\hat{\boldsymbol{d}}(t)$ as follows:

$$\begin{aligned}\dot{\hat{\boldsymbol{d}}} &= \dot{\xi} + \boldsymbol{K}_0\dot{\boldsymbol{G}}^{-1}(\boldsymbol{x}_1)\boldsymbol{x}_2 + \boldsymbol{K}_0\boldsymbol{G}^{-1}(\boldsymbol{x}_1)\dot{\boldsymbol{x}}_2 = -\boldsymbol{K}_0\xi - \boldsymbol{K}_0(\dot{\boldsymbol{G}}^{-1}(\boldsymbol{x}_1)\boldsymbol{x}_2 \\ &\quad + \boldsymbol{G}^{-1}(\boldsymbol{x}_1)\boldsymbol{F}_2(\boldsymbol{x}_1,\boldsymbol{x}_2,\boldsymbol{u}) + \boldsymbol{K}_0\boldsymbol{G}^{-1}(\boldsymbol{x}_1)\boldsymbol{x}_2) + \boldsymbol{K}_0\dot{\boldsymbol{G}}^{-1}(\boldsymbol{x}_1)\boldsymbol{x}_2 \\ &\quad + \boldsymbol{K}_0\boldsymbol{G}^{-1}(\boldsymbol{x}_1)(\boldsymbol{F}_2(\boldsymbol{x}_1,\boldsymbol{x}_2,\boldsymbol{u}) + \boldsymbol{G}(\boldsymbol{x}_1)\boldsymbol{d}(t)) = \boldsymbol{K}_0(\boldsymbol{d}(t) - \hat{\boldsymbol{d}}).\end{aligned} \tag{A.1}$$

Since $\boldsymbol{d}_e = \boldsymbol{d} - \hat{\boldsymbol{d}}$, using (A.1) we have

$$\dot{\boldsymbol{d}}_e = -\boldsymbol{K}_0\boldsymbol{d}_e + \dot{\boldsymbol{d}}(t). \tag{A.2}$$

Consider the Lyapunov function candidate

$$V_e = \tfrac{1}{2}\boldsymbol{d}_e^T\boldsymbol{d}_e, \tag{A.3}$$

whose first time derivative along the solutions of (A.2) satisfies

$$\dot{V}_e = -\boldsymbol{d}_e^T \boldsymbol{K_0} \boldsymbol{d}_e + \boldsymbol{d}_e^T \dot{\boldsymbol{d}} \le -(\lambda_{\min}(\boldsymbol{K_0})-\varepsilon)\boldsymbol{d}_e^T \boldsymbol{d}_e + \frac{1}{4\varepsilon}\dot{\boldsymbol{d}}^T \dot{\boldsymbol{d}} \le -2(\lambda_{\min}(\boldsymbol{K_0})-\varepsilon)V_e + \frac{1}{4\varepsilon}C_d^2. \quad \text{(A.4)}$$

where $\lambda_{min}(\boldsymbol{K_0})$ is the minimum eigenvalue of the matrix $\boldsymbol{K_0}$; ε is a positive constant such that $\lambda_{min}(\boldsymbol{K_0})-\varepsilon$ is strictly positive; and we have used $|\boldsymbol{d}_e^T(t)\dot{\boldsymbol{d}}(t)| \le \varepsilon\|\boldsymbol{d}_e\|^2 + (1/4\varepsilon)\|\dot{d}(t)\|^2$. From (A.4), it is seen that V_e exponentially converges to a ball centered the origin with the radius $R_{Ve} = C_d^2/8\varepsilon(\lambda_{\min}(\boldsymbol{K_0})-\varepsilon)$ as long as the solutions $\boldsymbol{x_1}(t)$ and $\boldsymbol{x_2}(t)$ exist. The existence of the solutions $\boldsymbol{x_1}(t)$ and $\boldsymbol{x_2}(t)$ is to be guaranteed by the design of the control input $\boldsymbol{u}$. This in turn means that the disturbance error $\boldsymbol{d_e}(t)$ exponentially converges to a ball centered at the origin with the radius $R_{de} = \sqrt{(1/4\varepsilon(\lambda_{\min}(\boldsymbol{K_0})-\varepsilon))}C_d$. Since $\lambda_{\min}(\boldsymbol{K_0})$ can be chosen arbitrarily large by choosing the matrix $\boldsymbol{K_0}$, the radius R_{de} can be made arbitrarily small. In the case $C_d=0$, the radius $R_{Ve}=R_{de}=0$ meaning that the disturbance error $\boldsymbol{d_e}(t)$ exponentially converges to zero.

Appendix B. Proof of Theorem 5.1

We prove Theorem 5.1 in three steps. The first step is to prove that the closed loop system consisting of (31), (28), (36) and the fifth equation of (14) is forward complete. In the second, we prove exponential convergence of the tracking errors ($\boldsymbol{q_e}, \psi_e, u_e, r_e$) and disturbance observer errors $\boldsymbol{b_e}$ to zero. Finally, we prove boundedness of $\boldsymbol{v}$ in the third step.

Step 1: *Forward completeness of the closed loop system*. To prove that the closed loop system consisting of (31), (28), (36) and the fifth equation of (14) is forward complete, we consider the following Lyapunov function candidate:

$$W_1 = V_2 + \frac{\sigma_1}{2}\boldsymbol{b}_e^T \boldsymbol{b_e} + \sigma_2(\sqrt{1+\overline{v}^2}-1) \quad \text{(B.1)}$$

where σ_1 and σ_2 are positive constants to be chosen later. Let us investigate the term

$$W_{11} = \sqrt{1+\overline{v}^2}-1. \quad \text{(B.2)}$$

Differentiating (B.2) along the solutions of the fifth equation of (14) and using $|a-b| \ge |a|-|b|$ give

$$\dot{W}_{11} \le \frac{Y_{|v|v}}{m_{22}}\frac{|\overline{v}|\overline{v}^2}{\sqrt{\overline{v}^2+1}} + \frac{Y_v}{m_{22}}\frac{\overline{v}^2}{\sqrt{\overline{v}^2+1}} + \frac{1}{\sqrt{\overline{v}^2+1}}\left(\lambda_1\overline{v}^2|r| + \lambda_2|\overline{v}|r^2 + \frac{|Y_r|}{m_{22}}|\overline{v}||r| + \frac{m_{11}}{m_{22}}|u||r||\overline{v}| + \frac{|b_1|+|b_2|}{m_{22}}|\overline{v}|\right), \quad \text{(B.3)}$$

where

$$\lambda_1 = \frac{1}{m_{22}}(2|\varepsilon Y_{|v|v}| + |Y_{|r|v}| + |Y_{|v|r}|),$$
$$\lambda_2 = \frac{1}{m_{22}}(\varepsilon^2|Y_{|v|v}| + |\varepsilon|(|Y_{|r|v}| + |Y_{|v|r}|) + |Y_{|r|r}). \quad \text{(B.4)}$$

Substituting (12) into the first equation of (26) results in

$$\begin{bmatrix}\beta_u\\ \dot{\alpha}\end{bmatrix} = \boldsymbol{Q}^{-1}\left(-\boldsymbol{K_1}\boldsymbol{q_e} - \dot{\boldsymbol{R}}(-\psi_d)\boldsymbol{R}^{-1}(-\psi_d)\boldsymbol{q_e} + \boldsymbol{R}(-\psi_d)\begin{bmatrix}\dot{x}_d\\ \dot{y}_d\end{bmatrix} - \boldsymbol{R}(-\psi_d)\boldsymbol{R^{-1}}(-\psi_d)\boldsymbol{R}(\psi_e)\begin{bmatrix}f_1\\ f_2\end{bmatrix} + \boldsymbol{R}(-\psi_d)\begin{bmatrix}\sin(\psi)\\ \cos(\psi)\end{bmatrix}\overline{v}\right), \quad \text{(B.5)}$$

which after a simple calculation yields

$$\begin{bmatrix}\beta_u\\ \dot{\alpha}\end{bmatrix} = -\frac{1}{\det(\boldsymbol{Q})}\begin{bmatrix}f_1'\cos(f_3)+f_2'\sin(f_3)\\ 1\end{bmatrix}\overline{v} + \boldsymbol{Q}^{-1}\left(-\boldsymbol{K_1}\boldsymbol{q_e} - \dot{\boldsymbol{R}}(-\psi_d)\boldsymbol{R^{-1}}(-\psi_d)\boldsymbol{q_e} + \boldsymbol{R}(-\psi_d)\begin{bmatrix}\dot{x}_d\\ \dot{y}_d\end{bmatrix} - \boldsymbol{R}(-\psi_d)\boldsymbol{R^{-1}}(-\psi_d)\boldsymbol{R}(\psi_e)\begin{bmatrix}f_1\\ f_2\end{bmatrix}\right). \quad \text{(B.6)}$$

Therefore we have the following bounds:

$$|\beta_u| \le \frac{|f_1'|+|f_2'|}{\det(\boldsymbol{Q})}|\overline{v}| + a_{11}\|\boldsymbol{q_e}\| + a_{10},$$
$$|\dot{\alpha}| \le \frac{1}{\det(\boldsymbol{Q})} + a_{21}\|\boldsymbol{q_e}\| + a_{20}, \quad \text{(B.7)}$$

where a_{10}, a_{11}, a_{20} and a_{21} are nonnegative bounded constants depending on the upper bounds of $|\dot{x}_d|$, $|\dot{y}_d|$, $|f_1|$ and $|f_2|$. Also, from the second equation of (26), we have the following bound for β_r:

$$|\beta_r| \le k_2|\psi_e| + |\dot{\psi}_d| + |f_3'||\dot{\alpha}| \le k_2|\psi_e| + a_{31}\|\boldsymbol{q_e}\| + \frac{|f_3'|}{\det(\boldsymbol{Q})}|\overline{v}| + a_{30}, \quad \text{(B.8)}$$

where a_{30} and a_{31} are nonnegative bounded constants depending on the upper bounds of $|\dot{x}_d|$, $|\dot{y}_d|$, $|f_1|$ and $|f_2|$. By noting that $u = u_e + \beta_u$ and $r = r_e + \beta_r$, applying the bounds (B.7) and (B.8) to (B.3) gives

$$\dot{W}_{11} \le -\left(\frac{Y_{|v|v}}{m_{22}} - \frac{m_{11}}{m_{22}}\frac{|f_1'|+|f_2'|}{\det(\boldsymbol{Q})} - \frac{|f_3'|(|\lambda_1|+4|\lambda_2|)}{\det(\boldsymbol{Q})}\right)\frac{|\overline{v}|\overline{v}^2}{\sqrt{\overline{v}^2+1}} + \frac{Y_v}{m_{22}}\frac{\overline{v}^2}{\sqrt{\overline{v}^2+1}} + \frac{A_1\overline{v}^2}{\sqrt{\overline{v}^2+1}} + A_2\psi_e^2 + A_3\|\boldsymbol{q_e}\|^2 + A_4u_e^2 + A_5r_e^2 + \frac{A_0}{\sqrt{\overline{v}^2+1}}, \quad \text{(B.9)}$$

where A_i, $i=0,\ldots,5$ are nonnegative bounded constants depending on a_{10}, a_{11}, a_{20}, a_{21}, a_{30} and a_{31}.

Now differentiating both sides of (B.1) along the solutions of (35), (31) and (B.9) results in

$$\begin{aligned}\dot{W}_1 \le\; & -\boldsymbol{q}_e^T\boldsymbol{K_1}\boldsymbol{q_e} - k_2\psi_e^2 - k_2\boldsymbol{q}_e^T\boldsymbol{\Delta_2}\psi_e - k_3u_e^2 - \rho_3\left(\frac{\partial\beta_u}{\partial\overline{v}}\right)^2u_e^2 - k_4r_e^2\\ & -\rho_4\left(\frac{\partial\beta_r}{\partial\overline{v}}\right)^2r_e^2 + \frac{u_e}{m_{11}}(b_{1e}\cos(\psi) + b_{2e}\sin(\psi))\\ & -\frac{\partial\beta_u}{\partial\overline{v}}\frac{u_e}{m_{22}}(-b_{1e}\sin(\psi) + b_{2e}\cos(\psi)) + \frac{m_{23}r_e}{\Delta}(b_{1e}\sin(\psi)\\ & -b_{2e}\cos(\psi)) + \frac{m_{22}r_e}{\Delta}b_{3e} - \frac{\partial\beta_r}{\partial\overline{v}}\frac{r_e}{m_{22}}(-b_{1e}\sin(\psi) + b_{2e}\cos(\psi))\\ & -\sigma_1\boldsymbol{b}_e^T\boldsymbol{K_0}\boldsymbol{b_e} + \sigma_1\boldsymbol{b_e}\dot{b}(t)\\ & -\sigma_2\left(\frac{Y_{|v|v}}{m_{22}} - \frac{m_{11}}{m_{22}}\frac{|f_1'|+|f_2'|}{\det(\boldsymbol{Q})} - \frac{|f_3'|(|\lambda_1|+4|\lambda_2|)}{\det(\boldsymbol{Q})}\right)\frac{|\overline{v}|\overline{v}^2}{\sqrt{\overline{v}^2+1}}\\ & +\sigma_2\frac{Y_v}{m_{22}}\frac{\overline{v}^2}{\sqrt{\overline{v}^2+1}} + \frac{A_1\overline{v}^2}{\sqrt{\overline{v}^2+1}} + \sigma_2A_2\psi_e^2 + \sigma_2A_3\|\boldsymbol{q_e}\|^2\\ & +\sigma_2A_4u_e^2 + \sigma_2A_5r_e^2 + \sigma_2\frac{A_0}{\sqrt{\overline{v}^2+1}}.\end{aligned} \quad \text{(B.10)}$$

Therefore by choosing the control design constants ε_i, $i=1, 2, 3$ such that

$$\frac{Y_{|v|v}}{m_{22}} - \frac{m_{11}}{m_{22}}\frac{|f_1'|+|f_2'|}{\det(\boldsymbol{Q})} - \frac{|f_3'|(|\lambda_1|+4|\lambda_2|)}{\det(\boldsymbol{Q})} \le -\lambda_0, \quad \text{(B.11)}$$

where λ_0 is a strictly positive constant, a simple calculation shows from (B.10) that

$$\dot{W}_1 \le C_1 W_1 + C_0, \tag{B.12}$$

where C_0 and C_1 are nonnegative bounded constants. The inequality (B.12) shows that the closed loop system consisting of (31), (28), (36) and the fifth equation of (14) is forward complete. Since the closed loop system is forward complete, we can now investigate stability of the subsystem $(\boldsymbol{q_e},\psi_e,u_e,r_e,\boldsymbol{b_e})$ and the subsystem $(\overline{v})$ separately in the following subsection.

Step 2: *Stability of* $(\boldsymbol{q_e},\psi_e,u_e,r_e,\boldsymbol{b_e})$ *subsystem*. To investigate stability of the $(\boldsymbol{q_e},\psi_e,u_e,r_e,\boldsymbol{b_e})$ subsystem, we consider the following Lyapunov function candidate:

$$W_2 = V_2 + \frac{\sigma_1}{2}\boldsymbol{b_e^T b_e} \tag{B.13}$$

whose derivative satisfies

$$\begin{aligned}\dot{W}_2 = &-\boldsymbol{q_e^T K_1 q_e} - k_2\psi_e^2 - k_2\boldsymbol{q_e^T}\boldsymbol{\Delta}_2\psi_e - k_3u_e^2 - \rho_3\left(\frac{\partial\beta_u}{\partial\overline{v}}\right)^2 u_e^2 - k_4r_e^2 \\ &-\rho_4\left(\frac{\partial\beta_r}{\partial\overline{v}}\right)^2 r_e^2 + \frac{u_e}{m_{11}}(b_{1e}\cos(\psi)+b_{2e}\sin(\psi)) \\ &-\frac{\partial\beta_u}{\partial\overline{v}}\frac{u_e}{m_{22}}(-b_{1e}\sin(\psi)+b_{2e}\cos(\psi)) + \frac{m_{23}r_e}{\Delta}(b_{1e}\sin(\psi) \\ &-b_{2e}\cos(\psi)) + \frac{m_{22}r_e}{\Delta}b_{3e} - \frac{\partial\beta_r}{\partial\overline{v}}\frac{r_e}{m_{22}}(-b_{1e}\sin(\psi)+b_{2e}\cos(\psi)) \\ &-\sigma_1\boldsymbol{b_e^T K_0 b_e}.\end{aligned} \tag{B.14}$$

By completing squares, we have

$$\dot{W}_2 \le -c_0 W_2, \tag{B.15}$$

where

$$\begin{aligned}c_0 = 2\min\Bigg(&(\lambda_{\min}(\boldsymbol{K_1}) - \varepsilon_1 k_2), \frac{k_2}{2}, \left(k_3 - \frac{a_1}{m_{11}}\right), \left(k_4 - \frac{|m_{23}a_2}{\Delta} - \frac{m_{22}a_3}{\Delta}\right), \\ &\left(\sigma_1\lambda_{\min}(\boldsymbol{K_0}) - \frac{1}{2m_{11}a_1} - \frac{1}{2\rho_3 m_{22}^2} - \frac{|m_{23}}{2\Delta a_3} - \frac{1}{2m_{22}^2\rho_4} - \frac{m_{22}}{4a_3\Delta}\right)\Bigg),\end{aligned} \tag{B.16}$$

where a_i, $i=1, 2, 3$ are positive constants. These constants are chosen such that c_0 is a strictly positive constant. This choice is always possible by picking sufficiently small a_i and a sufficiently large σ_1. The inequality (B.15) implies that $W_2(t) \le W_2(t_0)e^{-c_0(t-t_0)}$ for all $t \ge t_0 \ge 0$. Therefore the errors $\boldsymbol{q_e}(t)$, $\psi_e(t)$, $u_e(t)$, $r_e(t)$ and $\boldsymbol{b_e}(t)$ exponentially converge to zero. This in turn implies from the coordinate transformations (7) and (10) that the first inequality in (37) holds.

Step 3: *Boundedness of* $\boldsymbol{v}$. Since we have already proved that the errors $\boldsymbol{q_e}(t)$, $\psi_e(t)$, $u_e(t)$, $r_e(t)$ and $\boldsymbol{b_e}(t)$ exponentially converge to a ball centered at the origin, boundedness of $\overline{v}$ directly follows from (B.9). Boundedness of the ship velocities (u, v, r) follows by the coordinate transformations (7), (23), and boundedness of the virtual controls β_u and β_r, i.e., the second inequality in (37) holds.

References

Behal, A., Dawson, D.M., Dixon, W.E., Yang, F., 2002. Tracking and regulation control of an underactuated surface vessel with nonintegrable dynamics. IEEE Transactions on Automatic Control 47, 495–500.

Brockett, R.W., 1983. Asymptotic stability and feedback stabilization. In: Brockett, R.W., Millman, R.S., Sussmann, H.J. (Eds.), Differential Geometric Control Theory. Birkhauser, Boston, pp. 181–191.

Dixon, W.E., Dawson, D.M., Zergeroglu, E., 2001. Nonlinear Control of Wheeled Mobile Robots. Springer, London.

Do, K.D., Jiang, Z.P., Pan, J., 2002a. Underactuated ship global tracking under relaxed conditions. IEEE Transactions on Automatic Control 47, 1529–1536.

Do, K.D., Jiang, Z.P., Pan, J., 2002b. Universal controllers for stabilization and tracking of underactuated ships. Systems and Control Letters 47, 299–317.

Do, K.D., Jiang, Z.P., Pan, J., 2003. Robust global stabilization of underactuated ships on a linear course: State and output feedback. International Journal of Control 76, 1–17.

Do, K.D., Pan, J., 2003. Global waypoint tracking control of underactuated ships under relaxed assumptions. In: Proceedings of the 42nd IEEE Conference on Decision and Control, pp. 1244–1249.

Do, K.D., Pan, J., 2005. Global tracking of underactuated ships with nonzero off-diagonal terms. Automatica 41, 87–95.

Do, K.D., Pan, J., 2009. Control of Ships and Underwater Vehicles: Design for Underactuated and Nonlinear Marine Systems. Springer, London.

Encarnacao, P., Pacoal, A., Arcak, M., 2000. Path following for autonomous marine craft. In: Proceedings of the 5th IFAC Conference on Manoeuvring and Control of Marine Craft, pp. 117–122.

Fossen, T.I., 2002. Marine Control Systems. Marine Cybernetics, Trondheim, Norway.

Godhavn, J.M., Fossen, T.I., Berge, S., 1998. Nonlinear and adaptive backstepping designs for tracking control of ships. International Journal of Adaptive Control and Signal Processing 12, 649–670.

Jiang, Z.P., 2002. Global tracking control of underactuated ships by Lyapunov's direct method. Automatica 38, 301–309.

Jiang, Z.P., Nijmeijer, H., 1999. A recursive technique for tracking control of nonholonomic systems in chained form. IEEE Transactions on Automatic Control 44, 265–279.

Khalil, H., 2002. Nonlinear Systems. Prentice-Hall.

Krstic, M., Kanellakopoulos, I., Kokotovic, P., 1995. Nonlinear and Adaptive Control Design. Wiley, New York.

Lefeber, E., Pettersen, K.Y., Nijmeijer, H., 2003. Tracking control of an under-actuated ship. IEEE Transactions on Control Systems Technology 11, 52–61.

Lizarraga, D.A., 2004. Obstructions to the existence of universal stabilizers for smooth control systems. Mathematics of Control, Signals, and Systems 16, 255–277.

Morin, P., Samson, C., 2001. A characterization of the lie algebra rank condition by transverse periodic functions. SIAM Journal of Control Optimization 40, 1227–1249.

Morin, P., Samson, C., 2003. Practical stabilization of driftless systems on lie groups: the transverse function approach. IEEE Transactions on Automatic Control 48, 1496–1508.

Morin, P., Samson, C., 2006. Control with transverse functions and a single generator of underactuated mechanical systems. In: Proceedings of the 45th IEEE Conference on Decision and Control, pp. 6110–6115.

Papoulias, F.A., 1994. Cross track error and proportional turning rate guidance of marine vehicles. Journal of Ship Research 38, 123–132.

Papoulias, F.A., Oral, Z., 1995. Hopf bifurcations and nonlinear studies of gain margins in path control of marine vehicles. Applied Ocean Research 17, 21–32.

Perez, T., Blanke, M., 2002. Mathematical ship modelling for marine applications. Technical Report, Technical University of Denmark.

Pettersen, K.Y., Lefeber, E., 2001. Way-point tracking control of ships. In: Proceedings of the 40th IEEE Conference on Decision and Control, pp. 940–945.

Pettersen, K.Y., Nijmeijer, H., 2001. Underactuated ship tracking control: theory and experiments. International Journal of Control 74, 1435–1446.

Sira-ramirez, H., 1999. On the control of the underactuated ship: a trajectory planning approach. In: Proceedings of the 38th Conference on Decision and Control, pp. 2192–2197.

Skjetne, R., Fossen, T.I., 2001. Nonlinear maneuvering and control of ships. In: Proceedings of OCEANS 2001 MTS/IEEE Conference and Exhibition, pp. 1808–1815.

SNAME, 1950. The Society of Naval Architects and Marine Engineers. Nomenclature for treating the motion of a submerged body through a fluid. In: Technical and Research Bulletin No. 1-5.

Toussaint, G.J., Basar, T., Bullo, F., 2000a. H_∞−optimal tracking control techniques for nonlinear underactuated systems. In: Proceedings of the 39th IEEE Conference on Decision and Control, pp. 2078–2083.

Toussaint, G.J., Basar, T., Bullo, F., 2000b. Tracking for nonlinear underactuated surface vessels with generalized forces. In: Proceedings of the 2000 IEEE International Conference on Control Applications, pp. 355–360.

Wichlund, K.Y., Sordalen, O.J., Egeland, O., 1995. Control properties of under-actuated vehicles. In: Proceedings of the IEEE International Conference on Robotics and Automation, pp. 2009–2014.

Zhang, R., Chen, Y., Sun, Z., Sun, F., Xu, H., 2000. Path control of a surface ship in restricted waters using sliding mode. IEEE Transactions on Control Systems Technology 8, 722–732.